

Interaction times for damped heavy-ion collisions*

W. U. Schröder,[†] J. R. Birkelund, and J. R. Huizenga

Nuclear Structure Research Laboratory[†] and Departments of Chemistry and Physics, University of Rochester, Rochester, New York 14627

K. L. Wolf

Argonne National Laboratory, Argonne, Illinois 60439

V. E. Viola, Jr.

Department of Chemistry, University of Maryland, College Park, Maryland 20742

(Received 22 November 1976)

Angular-momentum dependent interaction times for damped heavy-ion reactions are deduced from experimental angular distributions. The angular momentum l is related to the experimental kinetic-energy loss assuming the energy loss to increase monotonically with decreasing l and the experimental cross section to be given by the sharp cutoff model. Although the analysis depends on the moment of inertia of the intermediate double-nucleus system, rather short interaction times are obtained ranging from 10^{-22} to several times 10^{-21} sec. Assuming this time scale, nucleon diffusion coefficients are deduced from experimental fragment charge distributions.

[NUCLEAR REACTIONS Deduced angular-momentum dependent interaction times and nucleon diffusion coefficients for reactions between very heavy ions.]

I. INTRODUCTION

Little information is available on the interaction time scale on which heavy-ion collisions occur with various degrees of kinetic energy damping. A knowledge of these interaction times is essential for an understanding of the mass, kinetic energy loss, and angular distributions of the reaction products from heavy ion collisions. This article is a report on angular-momentum dependent interaction times of heavy-ion reactions deduced from the cross section and the angular distributions measured as a function of the total kinetic energy loss. In addition, by assuming the validity of a diffusion model for nucleon transfer, diffusion coefficients are extracted from the measurements of Z distributions of the reaction fragments.

The experimental angular distributions integrated over mass (M) and total kinetic energy (TKE) of fragments from heavy-ion reactions depend markedly on the projectile-target combination and the bombarding energy.¹⁻¹¹ Correlations between mass, reaction angle, and kinetic energy of the fragments are exhibited in contour maps of (1) $d^2\sigma/d\theta dE$ on the E and θ plane,¹² (2) $d^2\sigma/dM d\theta$ on the M and θ plane, and (3) $d^2\sigma/dM dE$ on the M and E plane.

Mass and angular distributions are found to depend on the degree of energy damping.^{8,13} Small energy losses lead to angular distributions which are sideways peaked near the quarter-point angle and to narrow mass distributions, whereas events with large energy losses are characterized by forward-peaked or relatively flat angular distri-

butions and wide mass distributions. The apparent correlation between the shape of the angular distribution and the fragment charge (or mass)^{13,14} is a consequence of the degree of energy damping. Fragments with charges near that of the projectile have on the average small kinetic energy loss and angular distributions characteristic of very short lifetimes. If, however, fragments with Z similar to the projectile and large kinetic energy losses are chosen, these have angular distributions which correspond more nearly to those many Z units away from the projectile.¹³ Hence, the important criterion for determination of the angular distribution is the kinetic energy loss. Experimental evidence^{8,12} on fragment-mass distributions suggests that during the time the two constituents of the intermediate double-nucleus system interact with each other, a mass equilibration process proceeds which is accompanied by a damping of the relative kinetic energy into other degrees of freedom. Since the equilibration processes are not completed during the short interaction times encountered in collisions between the very heavy ions under consideration, the amount of kinetic energy lost signifies the stage of evolution of the system and, hence, the total interaction time experienced. This view is supported by classical dynamical calculations^{15,16} which show that the energy loss is a monotonic function of the initial angular momentum and the total interaction time. Associated with each interaction time is a Z distribution which is characterized by a variance σ_z^2 .

II. CLASSICAL MODEL FOR INTERACTION TIMES

Depending on the charge product $Z_T Z_P$ and the incident energy above the Coulomb energy, the ridge of highest cross section in a contour plot of type 1 may move forward, backward, or stay constant in angle as a function of kinetic energy loss. This latter behavior has been referred to as "strong focusing" of the angular distribution^{2,3,7} and suggests an angular-momentum dependence of the interaction time since many impact parameters lead to the same reaction angle.^{17,18} The present analysis assumes a monotonic increase in the total kinetic energy (TKE) loss with decreasing values of the impact parameter. For simplicity we employ a sharp cutoff model where the cross section for angular momenta up to l_j is given by $\sigma_j = \pi\lambda^2(l_j + 1)^2$. Using experimental results¹⁹ on the heavy-ion reaction cross section as a function of TKE loss, $d\sigma/d(\text{TKE loss})$, the angular momentum is related to the TKE loss by

$$l_i = [(l_j + 1)^2 - \Delta\sigma_{ij}/(\pi\lambda^2)]^{1/2} - 1, \quad (1)$$

where $\Delta\sigma_{ij} = \sigma_j - \sigma_i$ is the cross section in a TKE window $E_i \leq \text{TKE} \leq E_j$.

Starting with l_{\max} and zero TKE loss, a deflection function is constructed from the experimental

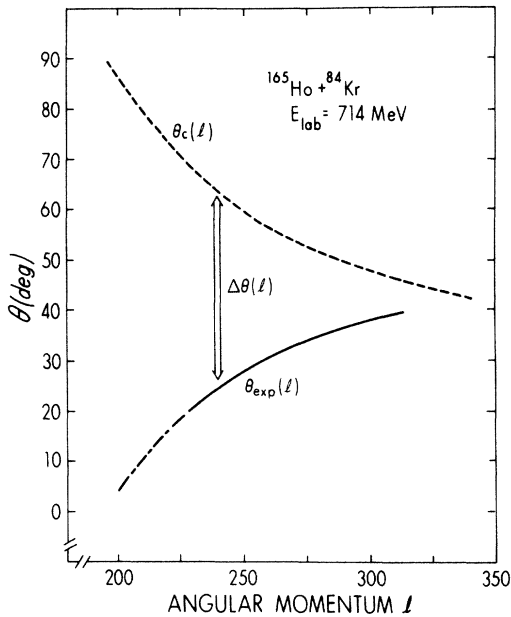


FIG. 1. Deflection functions for the reaction $^{165}\text{Ho} + ^{84}\text{Kr}$. The dashed curve is the Coulomb deflection function, calculated for the NS condition. The curve $\theta_{\text{exp}}(l)$ is the deflection function generated from experimental data (solid line) and extrapolated into an angular region where no data exist (long-short dashed line). $\Delta\theta(l)$ is the angle through which the intermediate double-nucleus system rotates during the interaction.

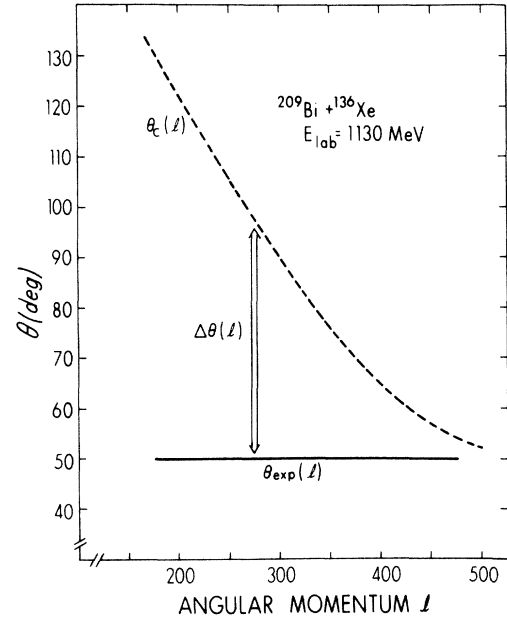


FIG. 2. Same as Fig. 1, but for the reaction $^{209}\text{Bi} + ^{136}\text{Xe}$.

data for a range of the higher l values. Examples of such deflection functions are shown as solid lines in Figs. 1 and 2 for the $^{165}\text{Ho} + ^{84}\text{Kr}$ ($E_{\text{lab}} = 714$ MeV) and $^{209}\text{Bi} + ^{136}\text{Xe}$ ($E_{\text{lab}} = 1130$ MeV) reactions, respectively. The plotted angles represent the angles where the cross section is at a maximum for a particular kinetic energy loss. In the above figures the kinetic energy loss has been converted to an angular momentum scale. For the first reaction the emission angle of the lighter fragment decreases as l decreases, whereas for the second reaction the emission angle is almost independent of l . For each reaction the energy damping and the variance in the Z distribution both increase as l decreases.

The angular momentum dependent interaction time is calculated with the expression^{17,18}

$$\tau(l) = \Delta\theta(l)g(l)/\hbar l, \quad (2)$$

where $\Delta\theta(l)$ is the difference between the Coulomb deflection angle $\theta_c(l)$ and the actual reaction angle $\theta_{\text{exp}}(l)$, and $g(l)$ is the moment of inertia of the double-nucleus system. The evaluation of $\tau(l)$ requires the adoption of a collision model. Here we present the results of calculations with two rather different models which are labeled as "nonsticking" (NS) and "sticking" (S) collisions. A sticking collision is defined by rigid rotation of the double-nucleus system as a whole. By a NS collision we specify that the entrance and exit channel orbital angular momenta are the same ($l_f = l_i$) and the

moment of inertia $\mathcal{I}_{\text{NS}} = \mu R^2$, where $\mu = M_1 M_2 / (M_1 + M_2)$, and R is the contact radius of the double-nucleus system (in the calculation the strong absorption radius²⁰ R_{SA} is used). In contrast to a nonsticking collision the interaction time for a sticking collision is calculated with \mathcal{I}_{NS} and the final orbital angular momentum where $l_f = (\mathcal{I}_{\text{NS}} / \mathcal{I}_{\text{S}}) l_i$ and $\mathcal{I}_{\text{S}} = \mathcal{I}_{\text{NS}} + \frac{2}{5} (M_1 R_1^2 + M_2 R_2^2)$. In the calculations presented, any variation in \mathcal{I}_{NS} with angular momentum or time is neglected. The Coulomb deflection function is estimated by $\theta_C(l_i) = 180^\circ - \psi_i(l_i) + \phi_i(l_i) - \psi_f(l_f) + \phi_f(l_f)$, where the symbols have been defined previously.¹⁸ In Figs. 1 and 2, Coulomb deflection functions are shown for the "nonsticking" (NS) model for the $^{165}\text{Ho} + ^{84}\text{Kr}$ ($E_{\text{lab}} = 714$ MeV) and $^{209}\text{Bi} + ^{136}\text{Xe}$ ($E_{\text{lab}} = 1130$ MeV) reactions, respectively.

Such a definition of the deflection during the reaction implies that no kinetic-energy loss due to dissipation or dynamical deformation effects occurs at separation distances larger than the strong-absorption radius R_{SA} . The agreement of realistic deflection function calculations²⁰ with experimental angular distributions for the heavy systems considered here suggests that the deviation of the trajectory with $l = l_{\text{max}}$ from a pure Coulomb trajectory is small. Hence, for $l < l_{\text{max}}$ the difference between Coulomb and observed deflection is used to evaluate the angle through which the intermediate system rotates during the nuclear interaction.

It should, however, be realized that it is impossible in principle to characterize the reaction between very heavy ions by a single deflection function. For such systems there are many intrinsic degrees of freedom coupled to the collective motion, and many different reaction paths may lead to similar values of a given experimental observable. Therefore, selecting a certain value of one experimental variable leads to a distribution of values of another variable fluctuating around its mean value. In this sense, the deflection functions derived above represent only average experimental deflection functions.

A relationship between experimental values of the total kinetic energy loss and the variance σ_z^2 of the fragment charge or Z distributions for very heavy-ion damped collisions has been reported previously.¹⁹ This relationship in conjunction with the experimental cross sections as a function of total kinetic-energy loss¹⁹ for various heavy-ion reactions is used to calculate angular momentum dependent values of the variance $\sigma_z^2(l)$. The value of $\sigma_z^2(l)$ is related to the interaction time $\tau(l)$ by application of a transport theory to multinucleon transfer processes. Assuming the occupation probabilities $P(Z, \tau)$ to be given by a Fok-

ker-Planck equation with constant coefficients leads to²¹

$$\sigma_z^2(l) = 2D_z(l)\tau(l). \quad (3)$$

The interpretation of the experimental fragment Z distributions in terms of Eq. (3) is subject to similar observations as made above for the construction of an experimental deflection function. The experimental variance σ_z^2 of the Z distribution is an average value determined by the range of l waves contributing to a given TKE window. A factorization of σ_z^2 according to Eq. (3) into mean values of D_z and τ applies only if $D_z(l)$ is a slowly varying function of both Z and l , because the above analysis suggests that the total interaction time $\tau(l)$ is a rapidly varying function decreasing exponentially with increasing l . This requirement on $D_z(l)$ seems, indeed, to be fulfilled as indicated by model calculations of Ayik, Schürmann, and Nörenberg²² and an experimentally observed small drift coefficient V_z , which is related to the diffusion coefficient according to the Einstein relation

$$V_z(l) = -\frac{1}{T} D_z \frac{\partial}{\partial Z} U_l(Z). \quad (4)$$

Here, T is the temperature of the system and $U_l(Z)$ is the potential energy for a fragmentation Z , both of which are slowly varying with Z and l .

The value $\tau(l)$ entering Eq. (3) is the mean value of the time during which the nucleon diffusion mechanism operates. In this analysis it is assumed that $\tau(l)$ is the total interaction time evaluated by the procedure outlined above. However, it is conceivable that nucleon diffusion occurs only during a part of this time although there is presently no experimental evidence for such a division of the total interaction time.

Values of $\tau(l)$ and $\sigma_z^2(l)$ determined for the $^{165}\text{Ho} + ^{84}\text{Kr}$ ($E_{\text{lab}} = 714$ MeV) and the $^{209}\text{Bi} + ^{136}\text{Xe}$ ($E_{\text{lab}} = 1130$ MeV) reactions are plotted in Figs. 3 and 4, respectively. The two different sets of values of $\tau(l)$ for each reaction in this figure are based on the above NS and S models. The interaction time corresponds to that period where the two heavy nuclei are in a close enough proximity to suffer a loss of kinetic energy and to exchange nucleons. The diffusion coefficient $D_z(l) = \sigma_z^2(l) / 2\tau(l)$ is rather independent of l for a particular choice of model, as illustrated by the lines drawn through the points in Figs. 3 and 4. However, for the sticking model (S) the points for the large angular momenta do not fall on a line through zero, indicating on the basis of Eq. (3) an initial increase in $D_z(l)$ as l decreases. The values of the diffusion coefficients for three heavy-ion reactions determined by the slope of the line fitted to the $\sigma_z^2(l)$ vs $\tau(l)$ data are given in Table I for each

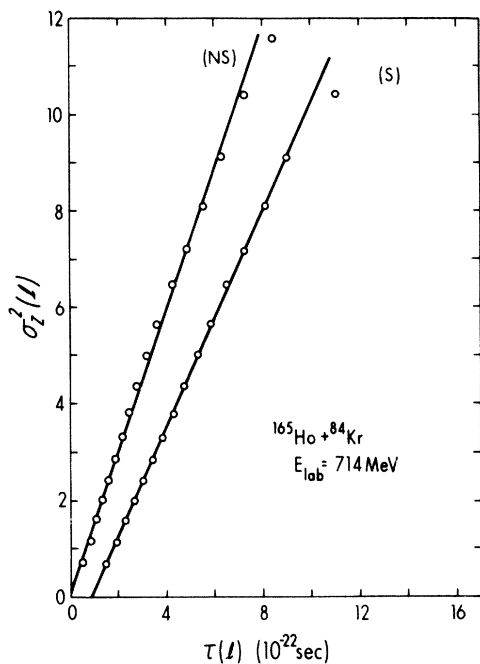


FIG. 3. The variance σ_z^2 of the experimental fragment-charge distribution plotted as a function of the interaction time τ for the reaction $^{165}\text{Ho} + ^{84}\text{Kr}$. The two sets of results correspond to the assumption of non-sticking (NS) or sticking (S) of the two ions during the interaction.

of the above two models. The proton number diffusion coefficient does not refer to proton diffusion alone, but to mass diffusion measured by the number of transferred protons. Assuming a conservation of the equilibrium Z/A ratio, the proton number (D_Z) and mass number (D_A) diffusion coefficients are related by $D_Z = (Z/A)^2 D_A$.

The present diffusion coefficients, based on an angular-momentum dependent interaction time,

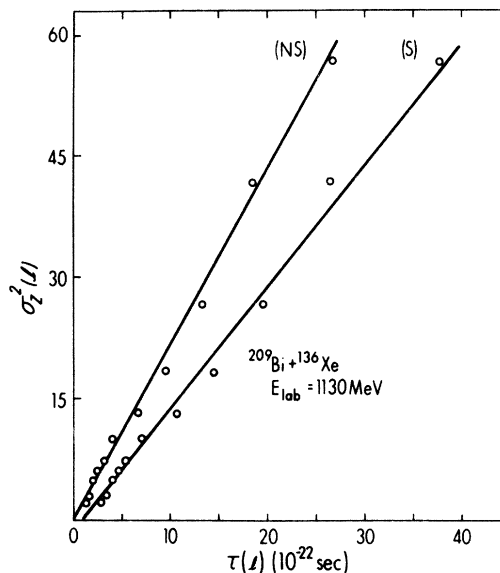


FIG. 4. Same as Fig. 3 but for the reaction $^{209}\text{Bi} + ^{136}\text{Xe}$.

are smaller (when comparisons are made for the same contact radius) than those reported by Nörenberg.²³ However, the difference is understood insofar that deflection functions were not employed in Ref. 23 and their resulting angle $\Delta\theta$ is too small. The value of D_Z for an average l value of $160\hbar$ for the $^{197}\text{Au} + ^{86}\text{Kr}$ reaction deduced by Moretto and Schmitt²⁴ at a laboratory energy of 620 MeV is comparable to our values for ^{84}Kr projectiles. The latter authors assume a sticking model and a Gaussian distribution of interaction times, the centroid of which varies linearly with l .

III. DISCUSSION

The results of the present analysis pose a number of questions with respect to the nature of the

TABLE I. Proton number (D_Z) and mass number (D_A) diffusion coefficients in units of 10^{22} sec^{-1} for Kr- and Xe-induced reactions. The proton number diffusion coefficient does *not* refer to proton diffusion alone, but to mass diffusion measured by the number of transferred protons; hence, $D_Z = (Z/A)^2 D_A$ for a constant Z/A ratio. The diffusion coefficients listed in this table are calculated from the *slopes* of lines drawn through plots of $\sigma_z^2(l)$ vs $\tau(l)$ over a range of l values. In the case of the sticking model, for example, the points for the highest l waves do not lie on a line which passes through the origin (see Figs. 3 and 4). *Individual values* of $D_Z(l)$ for the sticking model are l dependent and increase initially as l decreases. The Kr- and Xe-projectile energies (lab) are 714 and 1130 MeV, respectively. The errors in the diffusion coefficients are of the order of 30%. However, the values scale with the contact radius [see Eqs. (2) and (3)] which for the reported values is assumed to be the strong absorption radius R_{SA} (Ref. 20).

Reaction	Sticking model		Nonsticking model	
	D_Z	D_A	D_Z	D_A
$^{209}\text{Bi} + ^{136}\text{Xe}$	0.75	4.8	1.1	7.0
$^{209}\text{Bi} + ^{84}\text{Kr}$	0.62	3.7	0.87	5.3
$^{165}\text{Ho} + ^{84}\text{Kr}$	0.55	3.2	0.74	4.3

reaction mechanism:

1. Is there a unique energy loss mechanism connected with nucleon transfer, or is the interaction time deduced a sum of successive time periods during which different processes take place?
2. Can one draw any conclusion from Figs. 3 and 4 as to whether the moment of inertia of the double-nucleus system stays constant during the interaction or not?
3. Is the diffusion coefficient really independent of the angular momentum and, hence, of the degree of interpenetration of the two ions?

Examination of the available data¹⁹ shows a relatively high rate of energy loss at small kinetic-energy losses and this rate drastically decreases with increasing energy loss (i.e., decreasing l). However, the width of the fragment-charge distribution increases continuously with energy loss, starting from very small energy losses. Consequently, if there is a very fast energy dissipation mechanism, independent of mass transfer, it must be acting during only a short fraction of the total interaction time in order to allow a nucleon diffusion process to evolve in such a continuous fashion. Furthermore, it must be less important for high l values. In this analysis, only the total interaction time is deduced, assuming the total energy loss is a monotonically decreasing function of l . The presence of a fast energy dissipation mechanism would not markedly change the time scale derived in the present analysis.

In Fig. 5 is plotted the ratio of the total kinetic energy (TKE) loss to the average number of nucleons exchanged as a function of the total kinetic energy loss. In a random walk process the average number of nucleons exchanged or the number of steps is given by a quantity related to the variance of the charge distribution, namely, $(A/Z)\sigma_z^2$. Hence, the ordinate in Fig. 5 is equivalent to the average kinetic energy loss per nucleon exchanged which we define as Δ . It is, of course, important to differentiate between the total number of nucleons exchanged and the net nucleon transfer which gives the final mass distribution. One sees from the results plotted in Fig. 5 that the average kinetic energy loss per exchanged nucleon decreases linearly as the total kinetic energy loss increases. Although these experimental energy-averaged values of Δ are not directly comparable to the excitation energy dependent theoretical quantities estimated by Ayik *et al.*^{22,25} the values for small excitation energy, where the comparison is allowed, are of the same order of magnitude.

Questions (2) and (3) are connected to each other, since they both refer to the fact that the experimental points follow a straight line when plotted as a σ_z^2 vs τ graph. Although this result is con-

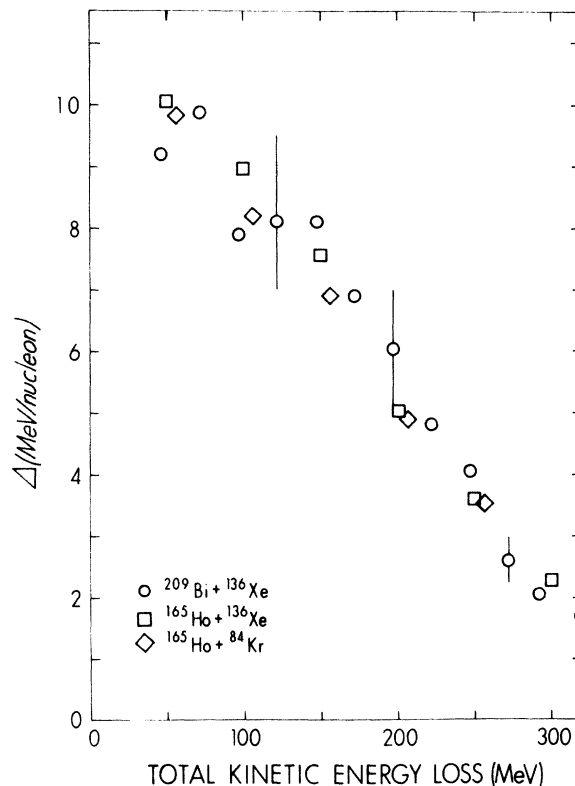


FIG. 5. Dependence of Δ (MeV/amu) on the total kinetic energy (TKE) loss. The values of Δ are calculated by dividing the total kinetic energy loss by $(A/Z)\sigma_z^2$. Adopting a diffusion model, this ratio is equivalent to the average energy lost per exchanged nucleon.

sistent with the view that the moment of inertia \mathcal{I} is constant during a significant part of the interaction and that the diffusion coefficient D is independent of l , other interpretations are not excluded. A change in \mathcal{I} would also imply a change in $\Delta\theta(l)$ [see Eq. (2)] leading, in general, to a nonlinear function $\sigma_z^2(\tau)$ and an l -dependent diffusion coefficient. However, the results for the NS and S models exhibited in Figs. 3 and 4 represent two extreme situations, of which the NS model is more appropriate, at least for a portion of the highest l values. However, as l decreases, the NS model may become less applicable. A transition from a NS model for large l to a S model for the smaller l analyzed here leads to a decrease in D_z with decreasing l .

In summary, interaction times increasing with decreasing angular momentum l are deduced for very heavy-ion reactions using a simple classical reaction model and assuming the kinetic-energy loss to decrease with increasing l . An alternate procedure would be a full trajectory calculation

including a frictional force.²⁶ The resulting interaction times turn out to be rather short, of the order 10^{-22} to several times 10^{-21} sec, indicating that caution has to be exercised in applying statistical models to the shorter lifetime processes. The l dependence of the interaction time is interpreted to be due to the delicate balance between repulsive Coulomb and attractive nuclear forces, which depends on the penetration depth of the trajectory and, hence, on the l value. This view leads to a natural understanding of the phenomena encountered in damped heavy-ion reactions. The angular distribution of the reaction cross section for a given projectile-target system viewed in a Wilczyński plot of $d^2\sigma/d\theta dE$ is expected to show the following dependence on the bombarding energy: The ridge of maximum cross section as a

function of energy loss will move more forward in angle with increasing bombarding energy for a given l wave, since the interaction times become longer with increasing penetration depth. The above model explains the variety of shapes of the angular distributions observed for a given system at different bombarding energies, including the occurrence of "angular focusing" at a particular energy. In this picture, negative-angle scattering or "orbiting" is anticipated for any system at a high enough bombarding energy. One concludes that, in general, a wide range of interaction times contributes to events at a particular reaction angle. The procedure which is outlined in this article represents a way to decompose experimental angular distributions with respect to the interaction time.

*Work supported by the U.S. Energy Research and Development Administration.

†Supported in part by a grant from the German Academic Exchange Service DAAD.

‡Supported by a grant from the National Science Foundation.

¹A. G. Artukh, G. F. Gridnev, V. L. Mikheev, V. V. Volkov, and J. Wilczyński, Nucl. Phys. A211, 299 (1973); A215, 91 (1973).

²F. Hanappe, M. Lefort, C. Ngô, J. Péter, and B. Tamain, Phys. Rev. Lett. 32, 738 (1974).

³K. L. Wolf, J. P. Unik, J. R. Huizenga, J. R. Birkelund, H. Freiesleben, and V. E. Viola, Phys. Rev. Lett. 33, 1105 (1974).

⁴J. Galin, L. G. Moretto, R. Babinet, R. Schmitt, R. Jared, and S. G. Thompson, Nucl. Phys. A255, 472 (1975).

⁵R. Babinet, L. G. Moretto, J. Galin, R. Jared, J. Moulton, and S. G. Thompson, Nucl. Phys. A258, 172 (1976).

⁶B. Tamain, F. Plasil, C. Ngô, J. Péter, M. Berlinger, and F. Hanappe, Phys. Rev. Lett. 36, 18 (1976).

⁷R. Vandenbosch, M. P. Webb, and T. D. Thomas, Phys. Rev. Lett. 36, 459 (1976); Phys. Rev. C 14, 143 (1976).

⁸W. U. Schröder, J. R. Birkelund, J. R. Huizenga, K. L. Wolf, J. P. Unik, and V. E. Viola, Phys. Rev. Lett. 36, 514 (1976).

⁹K. L. Wolf, J. R. Huizenga, J. R. Birkelund, H. Freiesleben, and V. E. Viola, Bull. Am. Phys. Soc. 21, 31 (1976); K. L. Wolf and C. T. Roche, in Proceedings of the Symposium on Macroscopic Features of Heavy-Ion Collisions [Argonne National Laboratory Report No. NAL/PHY-76-2, 1976 (unpublished)], Vol. I, p. 295.

¹⁰M. P. Webb, R. Vandenbosch, and T. D. Thomas, Phys. Lett. 62B, 407 (1976).

¹¹R. Vandenbosch, M. P. Webb, T. D. Thomas, and M. S. Zisman, Nucl. Phys. A269, 210 (1976).

¹²J. Wilczyński, Phys. Lett. 47B, 484 (1973).

¹³J. R. Birkelund, J. R. Huizenga, W. U. Schröder, H. Freiesleben, K. L. Wolf, J. P. Unik, and V. E.

Viola (unpublished); J. R. Huizenga, ERDA Progress Report No. COO-3496-56, 1976 (unpublished), p. 88.

¹⁴L. G. Moretto, B. Gauvin, P. Glässel, R. Jared, P. Russo, J. Sventek, and G. Wozniak, Phys. Rev. Lett. 36, 1069 (1976).

¹⁵K. Siwek-Wilczyńska and J. Wilczyński, Nucl. Phys. A264, 115 (1976).

¹⁶D. H. E. Gross, H. Kalinowski, and J. N. De, in *Symposium on Classical and Quantum Mechanical Aspects of Heavy Ion Collisions, Heidelberg, 1974* (Springer-Verlag Lecture Notes in Physics, 1975), Vol. 33, p. 194.

¹⁷J. R. Huizenga, Nukleonika 20, 291 (1975).

¹⁸J. P. Bondorf, J. R. Huizenga, M. I. Sobel, and D. Sperber, Phys. Rev. C 11, 1265 (1975).

¹⁹J. R. Huizenga, J. R. Birkelund, W. U. Schröder, K. L. Wolf, and V. E. Viola, Phys. Rev. Lett. 37, 885 (1976).

²⁰J. R. Huizenga, J. R. Birkelund, and W. Johnson, in Symposium on Macroscopic Features of Heavy-Ion Collisions [Argonne National Laboratory Report No. ANL-PHY-76-2, 1976 (unpublished)], Vol. I, p. 1.

²¹W. Nörenberg, Phys. Lett. 52B, 289 (1975).

²²S. Ayik, B. Schürmann, and W. Nörenberg, Z. Phys. A279, 145 (1976).

²³W. Nörenberg, in Proceedings of the European Conference on Nuclear Physics with Heavy Ions, Caen, 1976 [J. Phys. (Paris), Colloque No. 5, C5-141].

²⁴L. G. Moretto and R. Schmitt, in Proceedings of the European Conference on Nuclear Physics with Heavy Ions, Caen, 1976 (see Ref. 23), p. 109.

²⁵S. Ayik, B. Schürmann, and W. Nörenberg, Z. Phys. A277, 299 (1976).

²⁶J. P. Bondorf, M. I. Sobel, and D. Sperber, Phys. Rep. 15C, 83 (1974); D. H. E. Gross, H. Kalinowski, and R. Beck, in *Proceedings of the International Conference on Nuclear Physics, Munich, 1973*, edited by J. de Boer and H. J. Mang (North-Holland, Amsterdam/American Elsevier, New York, 1973); Phys. Lett. 48B, 302 (1974).